CHAPTER 7. THE GREENHOUSE EFFECT

We examine in this chapter the role played by atmospheric gases in controlling the temperature of the Earth. The main source of heat to the Earth is solar energy, which is transmitted from the Sun to the Earth by *radiation* and is converted to heat at the Earth's surface. To balance this input of solar radiation, the Earth itself emits radiation to space. Some of this terrestrial radiation is trapped by *greenhouse gases* and radiated back to the Earth, resulting in the warming of the surface known as the *greenhouse effect.* As we will see, trapping of terrestrial radiation by naturally occurring greenhouse gases is essential for maintaining the Earth's surface temperature above the freezing point.

There is presently much concern that anthropogenic increases in greenhouse gases could be inducing rapid surface warming of the Earth. The naturally occurring greenhouse gases CO_2, CH_4, and N_2O show large increases over the past century due to human activity (Figure 7-1). The increase of CO_2 was discussed in chapter 6, and the increases of CH_4 and N_2O will be discussed in chapters 11 and 10 respectively. Additional greenhouse gases produced by the chemical industry, such as CFC-11, have also accumulated in the atmosphere over the past decades and added to the greenhouse effect (Figure 7-1).
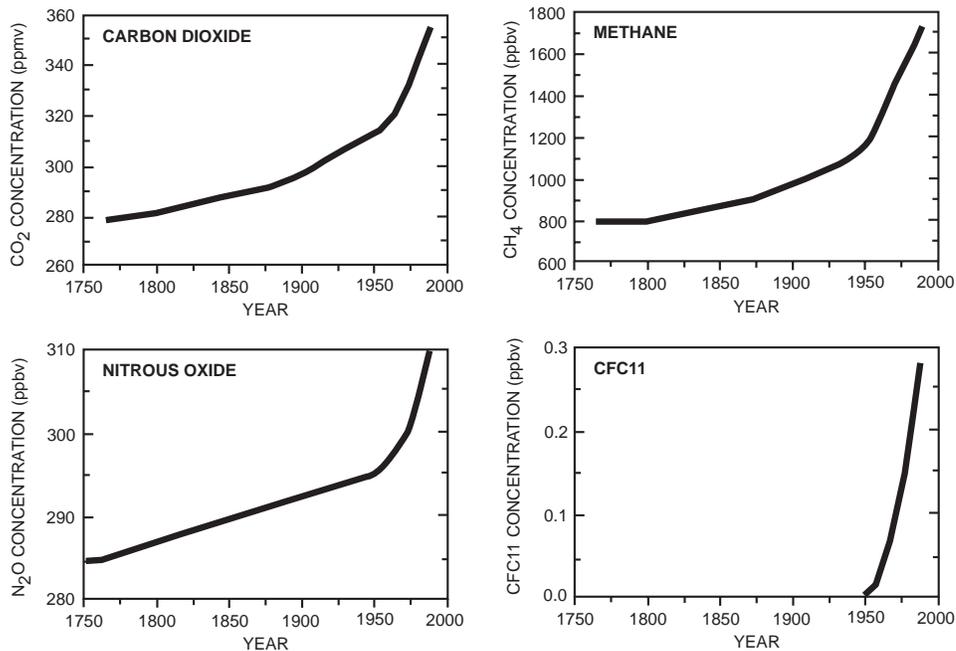

Figure 7-1 Rise in the concentrations of greenhouse gases since the 18th century

As we will see in section 7.3, simple theory shows that a rise in greenhouse gases should result in surface warming; the uncertainty lies in the magnitude of the response. It is well established that the global mean surface temperature of the Earth has increased over the past century by about 0.6 K. The evidence comes from direct temperature observations (Figure 7-2, top panel) and also from observations of sea-level rise and glacier recession. According to current climate models, this observed temperature rise can be explained by increases in greenhouse gases. The same models predict a further 1-5 K temperature rise over the next century as greenhouse gases continue to increase.
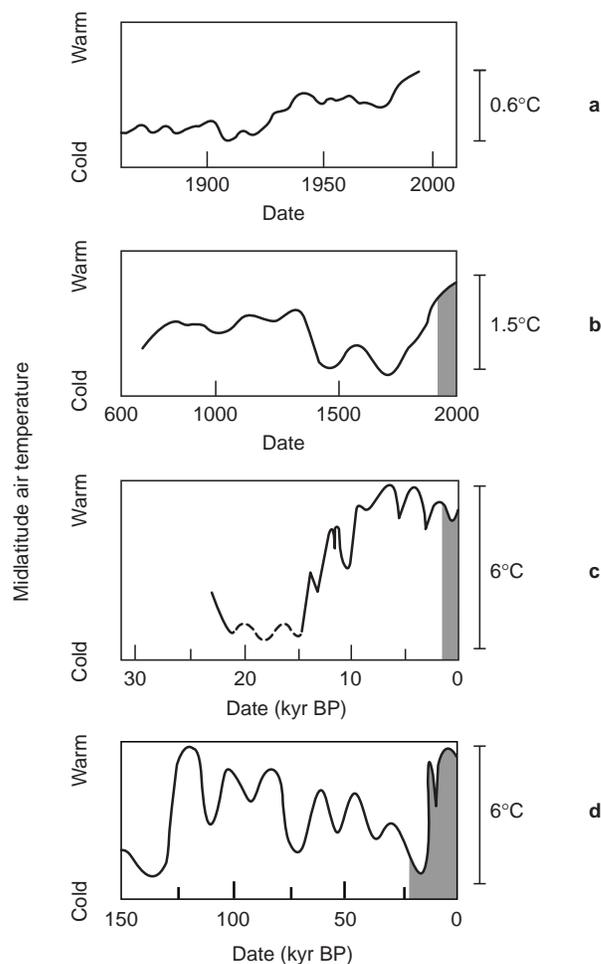

Figure 7-2 Trend in the surface temperature of the Earth at northern midlatitudes over the past 150,000 years. Each panel from the top down shows the trend over an increasingly longer time span, with the shaded area corresponding to the time span for the panel directly above. The record for the past 300 years is from direct temperature measurements and the longer-term record is from various proxies.
From Graedel, T.E., and P.J. Crutzen, *Atmospheric Change: an Earth System Perspective,* New York: Freeman, 1993.

Examination of the long-term temperature record in Figure 7-2 may instill some skepticism, however. Direct measurements of temperature in Europe date back about 300 years, and a combination of various proxies can provide a reliable thermometer extending back 150,000 years. From Figure 7-2 (second panel from top), we see that the warming observed over the past century is actually the continuation of a longer-term trend which began in about 1700 AD, before anthropogenic inputs of greenhouse gases became appreciable. This longer-term trend is thought to be caused by natural fluctuations in solar activity. Going back further in time we find that the surface temperature of the Earth has gone through large natural swings over the past 10,000 years, with temperatures occasionally higher than present (Figure 7-2, second panel from bottom). Again, fluctuations in solar activity may be responsible. Extending the record back to 150,000 years (Figure 7-2, bottom panel) reveals the succession of glacial and interglacial climates driven by periodic fluctuations in the orbit and inclination of the Earth relative to the Sun. From consideration of Figure 7-2 alone, it would be hard to view the warming over the past 100 years as anything more than a natural fluctuation! Nevertheless, our best understanding from climate models is that the warming is in fact due to increases in greenhouse gases. To explore this issue further, we need to examine the foundations and limitations of the climate models.

7.1 RADIATION

Radiation is energy transmitted by electromagnetic waves. All objects emit radiation. As a simple model to explain this phenomenon, consider an arbitrary object made up of an ensemble of particles continuously moving about their mean position within the object. A charged particle in the object oscillating with a frequency ν induces an oscillating electric field propagating outside of the object at the speed of light c (Figure 7-3). The oscillating electric field, together with the associated oscillating magnetic field, is an *electromagnetic wave* of wavelength $\lambda = c/\nu$ emitted by the object. The electromagnetic wave carries energy; it induces oscillations in a charged particle placed in its path. One refers to electromagnetic waves equivalently as *photons*, representing quantized packets of energy with zero mass traveling at the speed of light. We will use the terminology "electromagnetic waves" when we wish to stress the wave nature of radiation, and "photons" when we wish to emphasize its quantized nature.
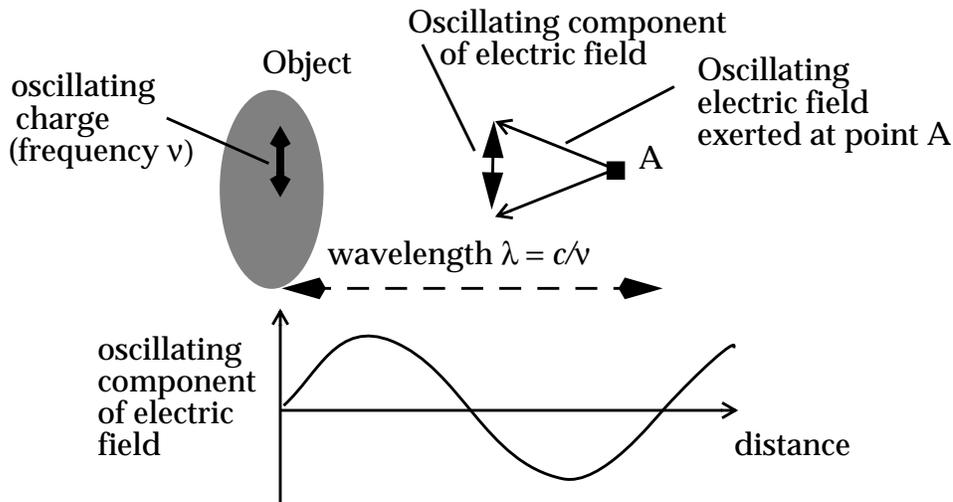
Figure 7-3 Electromagnetic wave induced by an oscillating charge in an object. The amplitude of the oscillating component of the electric field at point A has been greatly exaggerated.

A typical object emits radiation over a continuous spectrum of frequencies. Using a spectrometer we can measure the radiation flux $\Delta\Phi$ (W m^{-2}) emitted by a unit surface area of the object in a wavelength bin [λ, $\lambda + \Delta\lambda$]. This radiation flux represents the photon energy flowing perpendicularly to the surface. By covering the entire spectrum of wavelengths we obtain the *emission spectrum* of the object. Since $\Delta\Phi$ depends on the width $\Delta\lambda$ of the bins and this width is defined by the resolution of the spectrometer, it makes sense to plot the radiation spectrum as $\Delta\Phi/\Delta\lambda$ vs. λ, normalizing for $\Delta\lambda$ (Figure 7-4).
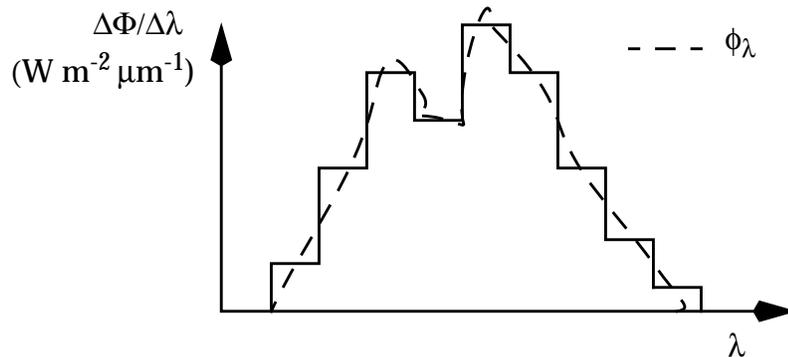

Figure 7-4 Emission spectrum of an object. The solid line is the flux measured by a spectrometer of finite wavelength resolution, and the dashed line is the corresponding flux distribution function.

Ideally one would like to have a spectrometer with infinitely high

resolution ($\Delta\lambda \rightarrow 0$) in order to capture the full detail of the emission spectrum. This ideal defines the *flux distribution function* ϕ_λ:

$$\phi_\lambda = \lim_{\Delta\lambda \rightarrow 0} \left(\frac{\Delta\Phi}{\Delta\lambda}\right) \qquad (7.1)$$

which is the derivative of the function $\Phi(\lambda)$ representing the total radiation flux in the wavelength range $[0, \lambda]$. The total radiation flux Φ_T emitted by a unit surface area of the object, integrated over all wavelengths, is

$$\Phi_T = \int_0^\infty \phi_\lambda \, d\lambda \qquad (7.2)$$

Because of the quantized nature of radiation, an object can emit radiation at a certain wavelength only if it absorbs radiation at that same wavelength. In the context of our simple model of Figure 7-3, a particle can emit at a certain oscillation frequency only if it can be excited at that oscillating frequency. A *blackbody* is an idealized object absorbing radiation of all wavelengths with 100% efficiency. The German physicist Max Planck showed in 1900 that the flux distribution function ϕ_λ^b for a blackbody is dependent only on wavelength and on the temperature T of the blackbody:

$$\phi_\lambda^b = \frac{2\pi h c^2}{\lambda^5 \left(\exp\left(\frac{hc}{kT\lambda}\right) - 1\right)} \qquad (7.3)$$

where $h = 6{,}63 \times 10^{-34}$ J s^{-1} is the Planck constant and $k = 1.38 \times 10^{-23}$ J K^{-1} is the Boltzmann constant. The function $\phi_\lambda^b(\lambda)$ is sketched in Figure 7-5. Three important properties are:

- Blackbodies emit radiation at all wavelengths.
- Blackbody emission peaks at a wavelength λ_{max} inversely proportional to temperature. By solving $\partial\phi_\lambda^b/\partial\lambda = 0$ we obtain $\lambda_{max} = \alpha/T$ where $\alpha = hc/5k = 2897$ μm K (*Wien's law).* This result makes sense in terms of our simple model: particles in a warmer object oscillate at higher frequencies.
- The total radiation flux emitted by a blackbody, obtained by integrating ϕ_λ^b over all wavelengths, is $\Phi_T = \sigma T^4$, where $\sigma = 2\pi^5 k^4/15c^2h^3 = 5.67 \times 10^{-8}$ W m^{-2} K^{-4} is the *Stefan-Boltzmann*
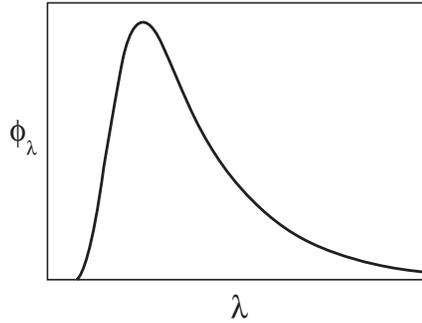
constant.

Figure 7-5 Flux distribution function for a blackbody

An alternate defintion of the flux distribution function is relative to the frequency $\nu = c/\lambda$:

$$\phi_\nu = \lim_{\Delta\nu \to 0}\left(\frac{\Delta\Phi}{\Delta\nu}\right) \tag{7.4}$$

where $\Delta\Phi$ is now the radiation flux in the frequency bin $[\nu, \nu + \Delta\nu]$. Yet another definition of the flux distribution function is relative to the *wavenumber* $\bar\nu = 1/\lambda = \nu/c$. The functions ϕ_ν and $\phi_{\bar\nu}$ are simply related by $\phi_{\bar\nu} = c\phi_\nu$. The functions ϕ_ν and ϕ_λ are related by

$$\phi_\nu = \left(\frac{d\lambda}{d\nu}\right)(-\phi_\lambda) = \frac{\lambda^2}{c}\phi_\lambda \tag{7.5}$$

For a blackbody,

$$\phi_\nu^b = \frac{2\pi h\nu^3}{c^2\left(\exp\left(\frac{h\nu}{kT}\right) - 1\right)} \tag{7.6}$$

Solution to $\partial\phi_\nu^b/\partial\nu = 0$ yields a maximum emission at frequency $\nu_{max} = 3kT/h$, corresponding to $\lambda_{max} = hc/3kT$. The function ϕ_ν peaks at a wavelength $5/3$ larger than the function ϕ_λ.

The Planck blackbody formulation for the emission of radiation is generalizable to all objects using *Kirchhoff's law*. This law states that if an object absorbs radiation of wavelength λ with an efficiency ε_λ, then it emits radiation of that wavelength at a fraction ε_λ of the corresponding blackbody emission at the same temperature. Using

Kirchhoff's law and equation *(7.3)*, one can derive the emission spectrum of any object simply by knowing its absorption spectrum and its temperature:

$$\phi_\lambda(T) = \varepsilon_\lambda(T)\phi_\lambda^b(T) \qquad (7.7)$$
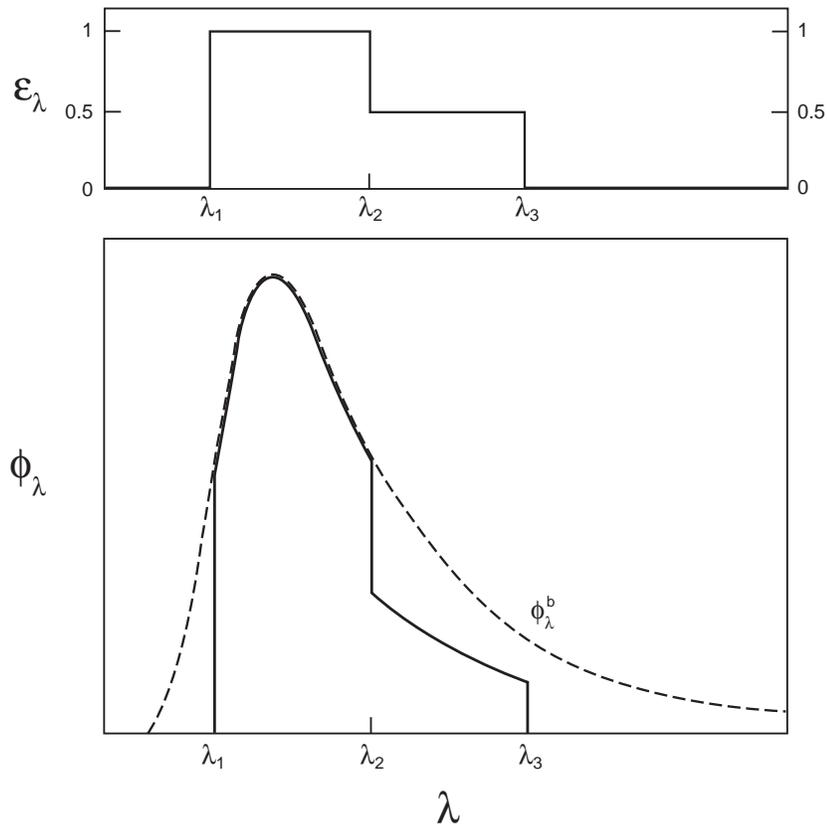
. An illustrative example is shown in Figure 7-6.

Figure 7-6 Radiation flux (solid line) emitted by an object that is transparent ($\varepsilon_\lambda = 0$) for wavelengths shorter than λ_1 or longer than λ_3, opaque ($\varepsilon_\lambda = 1$) for wavelengths between λ_1 and λ_2, and 50% absorbing ($\varepsilon_\lambda = 0.5$) for wavelengths between λ_2 and λ_3 The dashed line is the blackbody curve for the temperature of the object.

7.2   EFFECTIVE TEMPERATURE OF THE EARTH

7.2.1 Solar and terrestrial emission spectra

The spectrum of solar radiation measured outside the Earth's atmosphere (Figure 7-7) matches closely that of a blackbody at 5800 K. Thus the Sun is a good blackbody, and from the emission spectrum we can infer a temperature of 5800 K at the Sun's surface. Solar radiation peaks in the *visible* range of wavelengths ($\lambda = 0.4$-0.7

μm) and is maximum in the green (λ = 0.5 μm). About half of total solar radiation is at infra-red wavelengths (IR; λ > 0.7 μm) and a small fraction is in the ultraviolet (UV; λ < 0.4 μm).   The solar radiation flux at sea level is weaker than at the top of the atmosphere (Figure 7-7), in part because of reflection by clouds. There are also major absorption features by O_2 and O_3 in the UV and by H_2O in the IR.
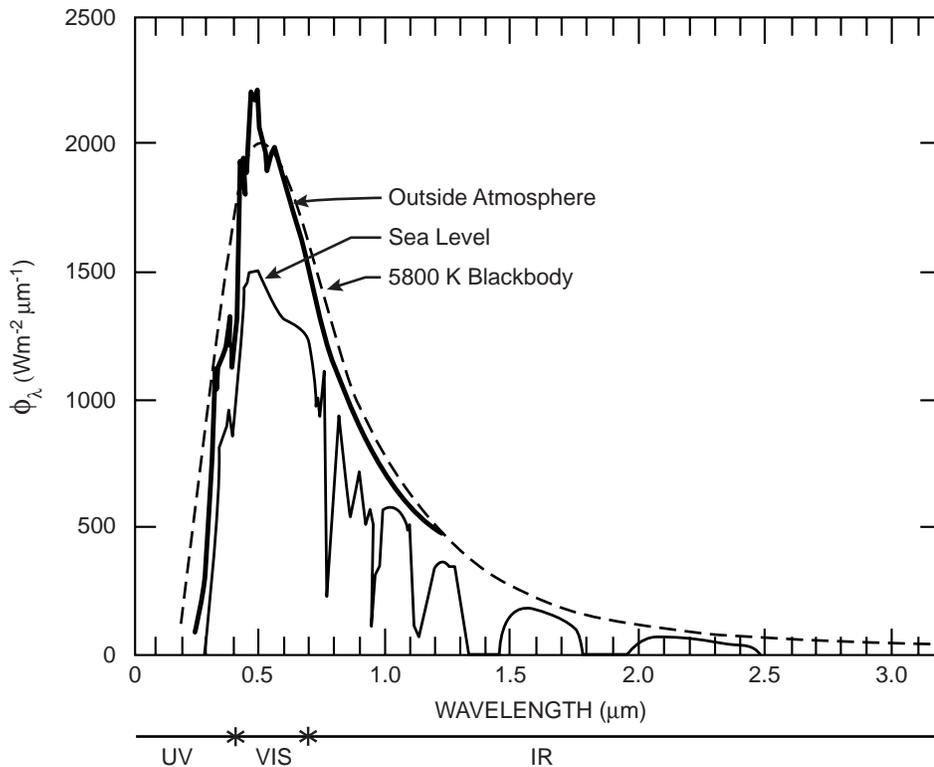

Figure 7-7 Solar radiation spectra measured from a satellite outside Earth's atmosphere (in bold) and at sea level.

A terrestrial radiation spectrum measured from a satellite over North Africa under clear-sky conditions is shown in Figure 7-8. As we will see in section 7.3.3, the terrestrial radiation spectrum is a combination of blackbody spectra for different temperatures, ranging from 220 to 320 K for the conditions in Figure 7-8. The wavelength range of maximum emission is 5-20 μm. The Earth is not sufficiently hot to emit significant amounts of radiation in the visible range (otherwise nights wouldn't be dark!).
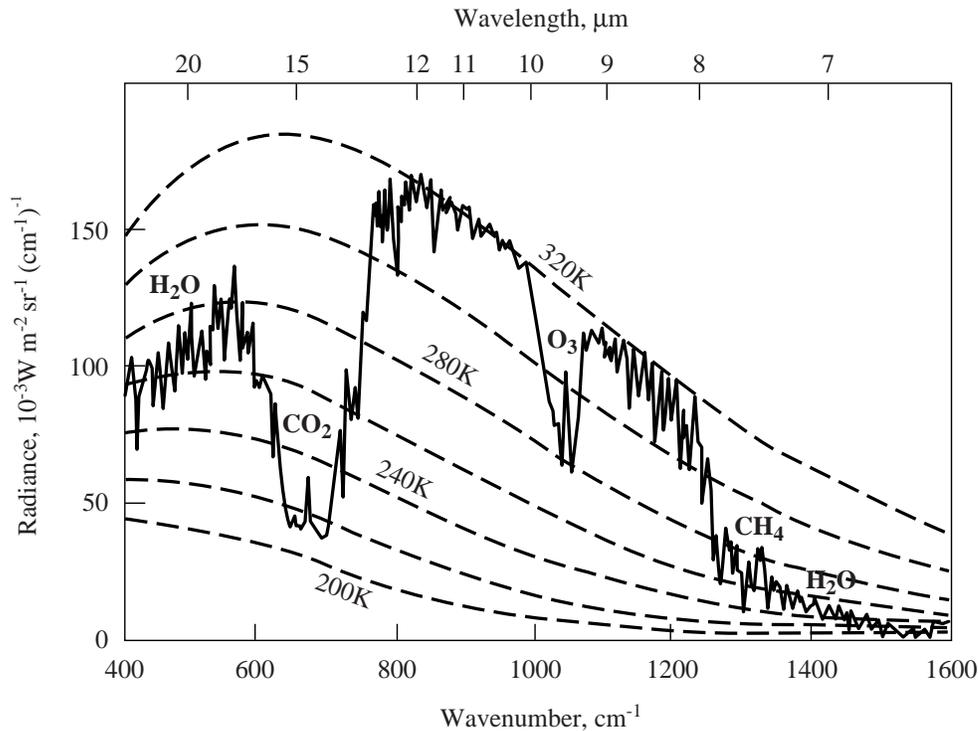
Wavelength, μm

Figure 7-8 Terrestrial radiation spectrum measured from a satellite over northern Africa (Niger valley) at noon. Blackbody curves for different temperatures are included for comparison. The plot shows radiances as a function of wavenumber ($\overline{\nu}$ = 1/λ). The radiance is the radiation energy measured by the satellite through a viewing cone normalized to unit solid angle (steradian, abbreviated sr). Radiance and $\phi_{\overline{\nu}}$ are related by a geometric factor. Major atmospheric absorbers are identified. Adapted from Hanel, R.A., et al., *J. Geophys. Res., 77,* 2629-2641, 1972.

7.2.2 Radiative balance of the Earth

In order to maintain a stable climate, the Earth must be in energetic equilibrium between the radiation it receives from the Sun and the radiation it emits out to space. From this equilibrium we can calculate the *effective temperature T_E* of the Earth.

The total radiation E_S emitted by the Sun (temperature T_S = 5800 K) per unit time is given by the radiation flux σT_S^4 multiplied by the area of the Sun:

$$E_S = 4\pi R_S^2 \sigma T_S^4 \qquad (7.8)$$

where $R_S = 7 \times 10^5$ km is the Sun's radius. The Earth is at a distance $d = 1.5 \times 10^8$ km from the Sun. The solar radiation flux F_S at that

distance is distributed uniformly over the sphere centered at the Sun and of radius *d* (Figure 7-9):

$$F_S = \frac{E_S}{4\pi d^2} = \frac{\sigma T_S^4 R_S^2}{d^2} \tag{7.9}$$
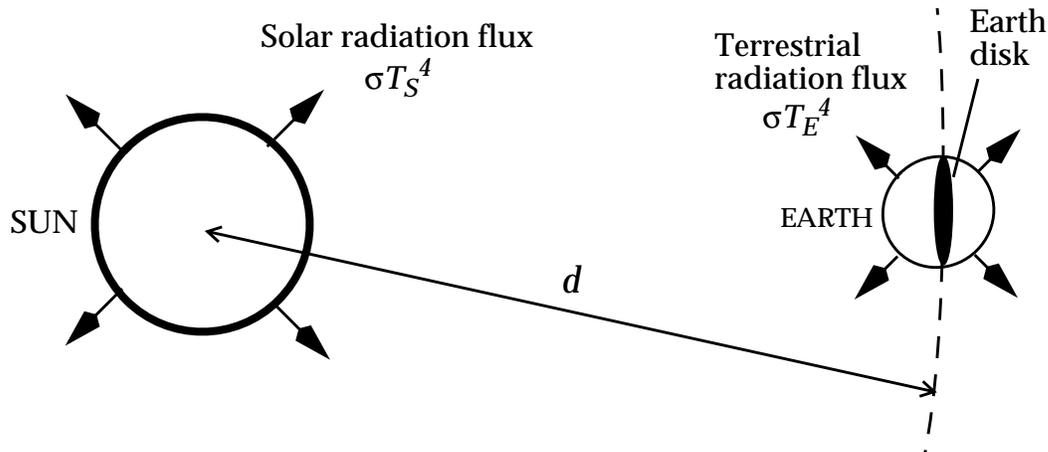

Figure 7-9 Radiative balance for the Earth

Substituting numerical values we obtain F_S = 1370 W m^{-2}. F_S is called the *solar constant* for the Earth. Solar constants for the other planets can be calculated from data on their distances from the Sun.

This solar radiation flux F_S is intercepted by the Earth over a disk of cross-sectional area πR_E^2 representing the shadow area of the Earth (Figure 7-9). A fraction *A* of the intercepted radiation is reflected back to space by clouds, snow, ice...; *A* is called the *planetary albedo.* Satellite observations indicate $A = 0.28$ for the Earth. Thus the solar radiation absorbed by the Earth per unit time is given by $F_S\pi R_E^2(1-A)$. The mean solar radiation flux absorbed per unit area of the Earth's surface is $F_S\pi R_E^2(1-A)/4\pi R_E^2 = F_S(1-A)/4$.

This absorption of energy by the Earth must be balanced by emission of terrestrial radiation out to space. The Earth is not a blackbody at visible wavelengths since the absorption efficiency of solar radiation by the Earth is only $\varepsilon = 1-A = 0.72$. However, the Earth radiates almost exclusively in the IR where the absorption efficiency is in fact near unity. For example, clouds and snow reflect visible radiation but absorb IR radiation. We approximate here the emission flux from the Earth as that of a blackbody of

temperature T_E, so that the energy balance equation for the Earth is

$$\frac{F_S(1-A)}{4} = \sigma T_E^4 \tag{7.10}$$

Rearrangement yields for the temperature of the Earth:

$$T_E = \left[\frac{F_S(1-A)}{4\sigma}\right]^{\frac{1}{4}} \tag{7.11}$$

Substituting numerical values we obtain T_E = 255 K. This seems a bit chilly if T_E is viewed as representing the surface temperature of the Earth. Instead we should view it as an *effective* temperature for the (Earth + atmosphere) system as would be detected by an observer in space. Some of the terrrestrial radiation detected by the observer may be emitted by the cold atmosphere rather than by the Earth's surface. In order to understand what controls the surface temperature of the Earth, we need to examine the radiative properties of the atmosphere.

Exercise 7-1 Venus is 1.08x10^6 km from the Sun; its albedo is 0.75. What is its effective temperature?

Answer. We calculate the solar constant F_S for Venus by using equation *(7.9)* with d = 1.08x10^6 km. We obtain F_S = 2640 W m^{-2}. Substituting in equation *(7.11)* with albedo A = 0.75 we obtain an effective temperature T = 232 K for Venus. Even though Venus is closer to the Sun than the Earth, its effective temperature is less because of the higher albedo. The actual surface temperature of Venus is 700 K due to an intense greenhouse effect (section 7.5).

7.3 ABSORPTION OF RADIATION BY THE ATMOSPHERE

7.3.1 Spectroscopy of gas molecules

A gas molecule absorbs radiation of a given wavelength only if the energy can be used to increase the internal energy level of the molecule. This internal energy level is quantized in a series of electronic, vibrational, and rotational states. An increase in the internal energy is achieved by transition to a higher state. Electronic transitions, that is, transitions to a higher electronic state,

generally require UV radiation (< 0.4 μm). Vibrational transitions require near-IR radiation (0.7-20 μm), corresponding to the wavelength range of peak terrestrial radiation. Rotational transitions require far-IR radiation (>20 μm). Little absorption takes place in the range of visible radiation (0.4-0.7 μm) which falls in the gap between electronic and vibrational transitions.

Gases that absorb in the wavelength range 5-50 μm, where most terrestrial radiation is emitted (Figure 7-8), are called *greenhouse gases*. The absorption corresponds to vibrational and vibrational-rotational transitions (a vibrational-rotational transition is one that involves changes in both the vibrational and rotational states of the molecule). A selection rule from quantum mechanics is that vibrational transitions are allowed only if the change in vibrational state changes the dipole moment p of the molecule. Vibrational states represent different degrees of stretching or flexing of the molecule, and an electromagnetic wave incident on a molecule can modify this flexing or stretching only if the electric field has different effects on different ends of the molecule, that is if $p \neq \mathbf{0}$. Examination of the geometry of the molecule can tell us whether a transition between two states changes p.

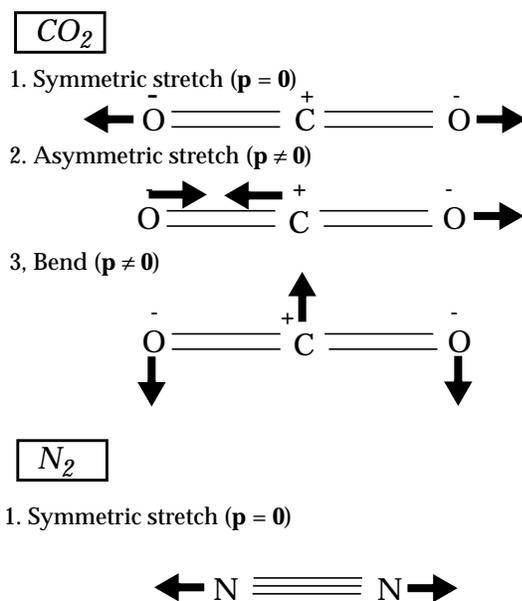**Figure 7-10 Normal vibrational modes of CO_2 and N_2**

Consider the CO_2 molecule (Figure 7-10). Its vibrational state is defined by a combination of three *normal* vibrational modes and by a quantized energy level within each mode. Vibrational transitions involve changes in the energy level (vibrational amplitude) of one of the normal modes (or rarely of a combination of normal modes).

In the "symmetric stretch" mode the CO_2 molecule has no dipole moment, since the distribution of charges is perfectly symmetric; transition to a higher energy level of that mode does not change the dipole moment of the molecule and is therefore forbidden. Changes in energy levels for the two other, asymmetric, modes change the dipole moment of the molecule and are therefore allowed. In this manner, CO_2 has absorption lines in the near-IR. Contrast the case of N_2 (Figure 7-10). The N_2 molecule has a uniform distribution of charge and its only vibrational mode is the symmetric stretch. Transitions within this mode are forbidden, and as a result the N_2 molecule does not absorb in the near-IR.

More generally, molecules that can acquire a charge asymmetry by stretching or flexing (CO_2, H_2O, N_2O, O_3, hydrocarbons...) are greenhouse gases; molecules that cannot acquire charge asymmetry by flexing or stretching (N_2, O_2, H_2) are not greenhouse gases. Atomic gases such as the noble gases have no dipole moment and hence no greenhouse properties. Examining the composition of the Earth's atmosphere (Table 1-1), we see that the principal constituents of the atmosphere (N_2, O_2, Ar) are not greenhouse gases. Most other constituents, found in trace quantities in the atmosphere, are greenhouse gases. The important greenhouse gases are those present at concentrations sufficiently high to absorb a significant fraction of the radiation emitted by the Earth; the list includes H_2O, CO_2, CH_4, N_2O, O_3, and chlorofluorocarbons (CFCs). By far the most important greenhouse gas is water vapor because of its abundance and its extensive IR absorption features.

The efficiency of absorption of radiation by the atmosphere is plotted in Figure 7-11 as a function of wavelength. Absorption is ~100% efficient in the UV due to electronic transitions of O_2 and O_3 in the stratosphere. The atmosphere is largely transparent at visible wavelengths because the corresponding photon energies are too low for electronic transitions and too high for vibrational transitions. At IR wavelengths the absorption is again almost 100% efficient because of the greenhouse gases. There is however a window between 8 and 13 μm, near the peak of terrestrial emission, where the atmosphere is only a weak absorber except for a strong O_3 feature at 9.6 μm. This *atmospheric window* allows direct escape of radiation from the surface of the Earth to space and is of great importance for defining the temperature of the Earth's surface.
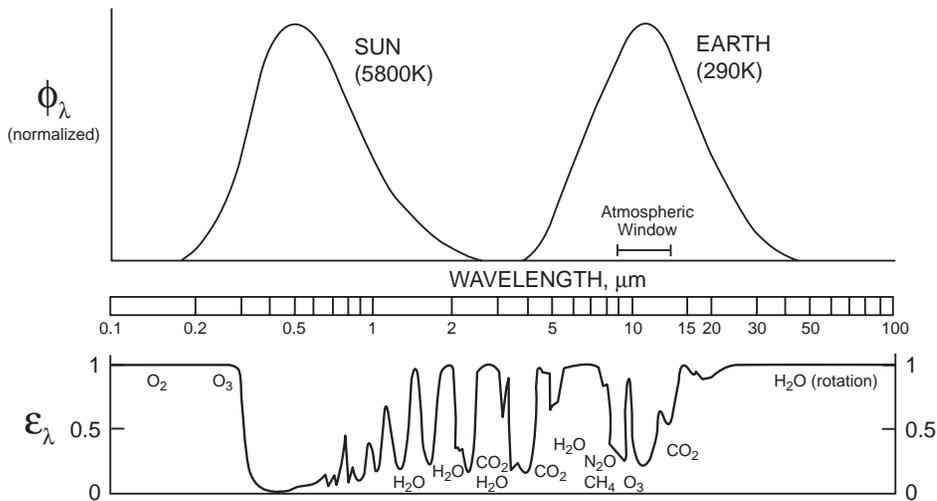
Figure 7-11 Efficiency of absorption of radiation by the atmosphere as a function of wavelength. Major absorbers are identified.

7.3.2 A simple greenhouse model

The concepts presented in the previous sections allow us to build a simple model of the greenhouse effect. In this model, we view the atmosphere as an isothermal layer placed some distance above the surface of the Earth (Figure 7-12). The layer is transparent to solar radiation, and absorbs a fraction f of terrestrial radiation because of the presence of greenhouse gases. The temperature of the Earth's surface is T_o and the temperature of the atmospheric layer is T_1.
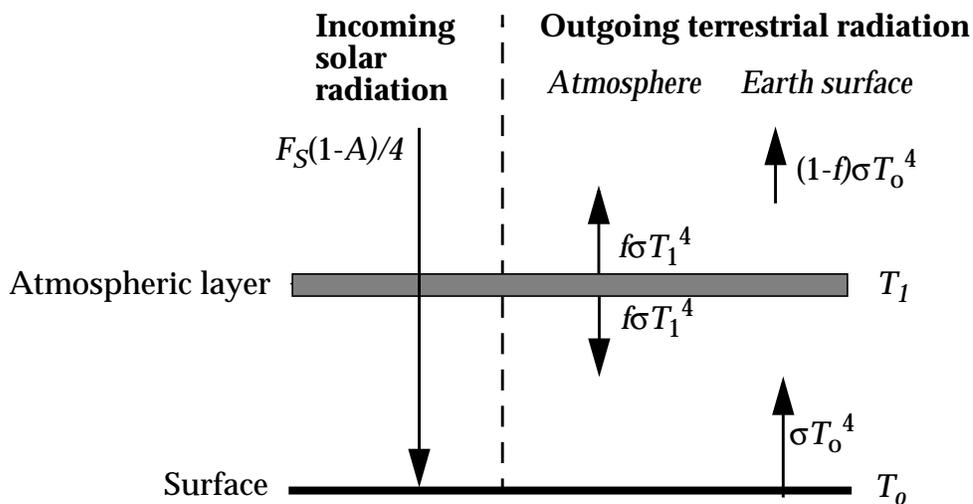

Figure 7-12 Simple greenhouse model. Radiation fluxes per unit area of Earth's surface are shown.

The terrestrial radiation flux absorbed by the atmospheric layer is $f\sigma T_0^4$. The atmospheric layer has both upward- and downward-facing surfaces, each emitting a radiation flux $f\sigma T_1^4$ (Kirchhoff's law). The energy balance of the (Earth + atmosphere) system, as viewed by an observer from space, is modified from equation *(7.10)* to account for absorption and emission of radiation by the atmospheric layer:

$$\frac{F_S(1-A)}{4} = (1-f)\sigma T_0^4 + f\sigma T_1^4 \tag{7.12}$$

A separate energy balance equation applies to the atmospheric layer:

$$f\sigma T_0^4 = 2 f\sigma T_1^4 \tag{7.13}$$

which leads to

$$T_0 = 2^{\frac{1}{4}} T_1 \tag{7.14}$$

Replacing *(7.13)* into *(7.12)* gives

$$\frac{F_S(1-A)}{4} = (1-f)\sigma T_0^4 + \frac{f}{2}\sigma T_0^4 = \left(1-\frac{f}{2}\right)\sigma T_0^4 \tag{7.15}$$

which we rearrange as

$$T_0 = \left[\frac{F_S(1-A)}{4\sigma\left(1-\frac{f}{2}\right)}\right]^{\frac{1}{4}} \tag{7.16}$$

The observed global mean surface temperature is $T_0 = 288$ K, corresponding to $f = 0.77$ in equation *(7.16)*. We can thus reproduce the observed surface temperature by assuming that the atmospheric layer absorbs 77% of terrestrial radiation. This result is not inconsistent with the data in Figure 7-11; better comparison would require a wavelength-dependent calculation. By substituting $T_0 = 288$ K into *(7.14)* we obtain $T_1 = 241$ K for the temperature of the atmospheric layer, which is roughly the observed temperature at the scale height $H = 7$ km of the atmosphere (Figure 2-2). Increasing concentrations of greenhouse

gases increase the absorption efficiency f of the atmosphere, and we see from equation *(7.16)* that an increase in the surface temperature T_0 will result.

We could improve on this simple greenhouse model by viewing the atmosphere as a vertically continuous absorbing medium, rather than a single discrete layer, applying the energy balance equation to elemental slabs of atmosphere with absorption efficiency *df(z)* proportional to air density, and integrating over the depth of the atmosphere. This is the classical "gray atmosphere" model described in atmospheric physics texts.   It yields an exponential decrease of temperature with altitude because of the exponential decrease in air density, and a temperature at the top of atmosphere of about 210 K which is consistent with typical tropopause observations (in the stratosphere, heating due to absorption of solar radiation by ozone complicates the picture). See problem 7. 5 for a simple derivation of the temperature at the top of the atmosphere. Radiative models used in research go beyond the gray atmosphere model by resolving the wavelength distribution of radiation, and *radiative-convective models* go further by accounting for buoyant transport of heat as a term in the energy balance equations.   Going still further are the *general circulation models* (GCMs) which resolve the horizontal heterogeneity of the surface and its atmosphere by solving globally the 3-dimensional equations for conservation of energy, mass, and momentum.   The GCMs provide a full simulation of the Earth's climate and are the major research tools used for assessing climate response to increases in greenhouse gases.

7.3.3 Interpretation of the terrestrial radiation spectrum

Let us now go back to the illustrative spectrum of terrestrial radiation in Figure 7-8. The integral of the terrestrial emission spectrum over all wavelengths, averaged globally, must correspond to that of a blackbody at 255 K in order to balance the absorbed solar radiation.   In our simple greenhouse model of section 7.3.2, this average is represented by adding the contributions of the emission fluxes from the warm surface and from the cold atmosphere *(equation (7.12))*. In the same manner, the spectrum in Figure 7-8 can be interpreted as a superimposition of blackbody spectra for different temperatures depending on the wavelength region (Figure 7-13). In the atmospheric window at 8-12 μm,the atmosphere is only weakly absorbing except for the O_3 feature at 9.6 μm. The radiation flux measured by a satellite in that wavelength range corresponds to a blackbody at the temperature of the Earth's surface, about 320 K for the spectrum in Figure 7-8.

Such a high surface temperature is not surprising considering that the spectrum was measured over northern Africa at noon.
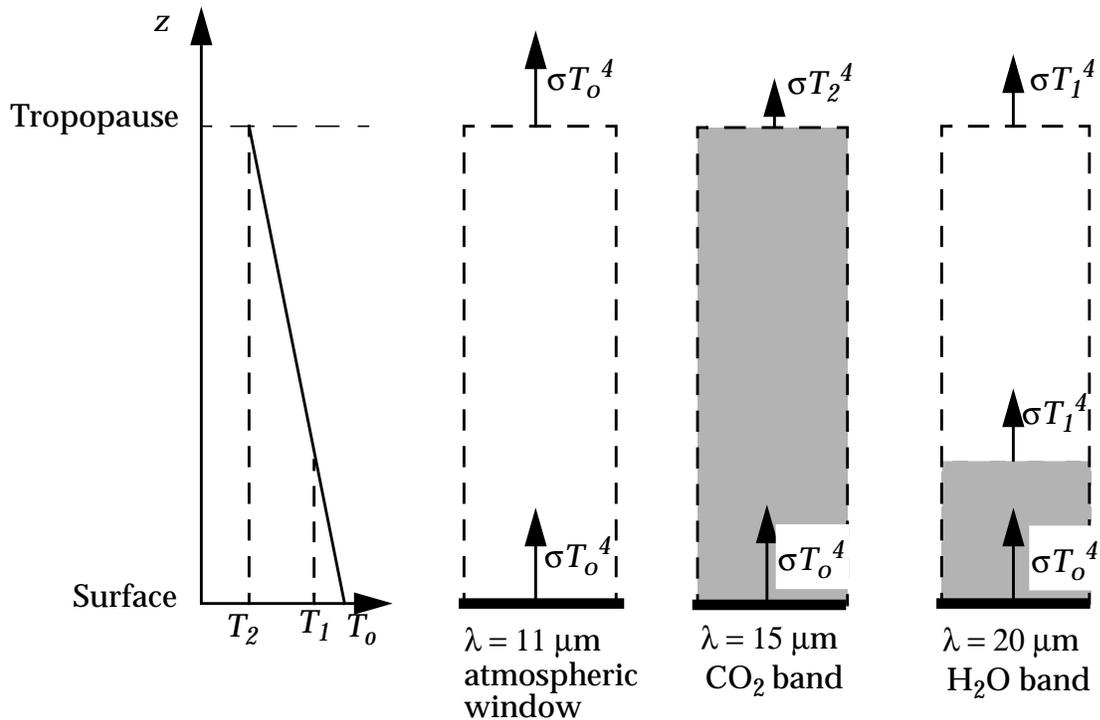

Figure 7-13 Radiation fluxes emitted to space at three different wavelengths and for the temperature profile in the left panel. Opaque regions of the atmosphere are shown in gray shading.

By contrast, in the strong CO_2 absorption band at 15 μm, radiation emitted by the Earth's surface is absorbed by atmospheric CO_2, and the radiation re-emitted by CO_2 is absorbed again by CO_2 in the atmospheric column. Because the atmosphere is opaque to radiation in this wavelength range, the radiation flux measured from space corresponds to emission from the altitude at which the CO_2 concentration becomes relatively thin, roughly in the upper troposphere or lower stratosphere. The 15 μm blackbody temperature in Figure 7-8 is about 215 K, which we recognize as a typical tropopause temperature.

Consider now the 20 μm wavelength where H_2O absorbs but not CO_2. The opacity of the atmosphere at that wavelength depends on the H_2O concentration. Unlike CO_2, H_2O has a short atmospheric lifetime and its scale height in the atmosphere is only a few kilometers (problem 5. 1). The radiation flux measured at 20 μm corresponds therefore to the temperature of the atmosphere at

about 5 kilometers altitude, above which the H_2O abundance is too low for efficient absorption (Figure 7-13).   This temperature is about 260 K for the example in Figure 7-8 .   The same emission temperature is found at 7-8 μm where again H_2O is a major absorber.

We see from the above discussion how terrestrial emission spectra measured from space can be used to retrieve information on the temperature of the Earth's surface as well as on the thermal structure and composition of the atmosphere.   Additional information on the vertical distribution of a gas can be obtained from the width of the absorption lines, which increase linearly with air density in the troposphere and lower stratosphere.   Research instruments aboard satellites use wavelength resolutions of the order of a nanometer to retrieve concentrations and vertical profiles of atmospheric gases, and intricate algorithms are needed for the retrieval.

Another important point from the above discussion is that all greenhouse gases are not equally efficient at trapping terrestrial radiation.   Consider a greenhouse gas absorbing at 11 μm, in the atmospheric window (Figure 7-8).   Injecting such a gas into the atmosphere would decrease the radiation emitted to space at 11 μm (since this radiation would now be emitted by the cold atmosphere rather than by the warm surface).   In order to maintain a constant terrestrial blackbody emission integrated over all wavelengths, it would be necessary to increase the emission flux in other regions of the spectrum and thus warm the Earth.   Contrast this situation to a greenhouse gas absorbing solely at 15 μm, in the CO_2 absorption band (Figure 7-8).   At that wavelength the atmospheric column is already opaque (Figure 7-13), and injecting an additional atmospheric absorber has no significant greenhouse effect.

7.4 RADIATIVE FORCING

We saw in section 7.3.2 how general circulation models (GCMs) can be used to estimate the surface warming associated with an increase in greenhouse gas concentrations.   The GCMs are 3-dimensional meteorological models that attempt to capture the ensemble of radiative, dynamical, and hydrological factors controlling the Earth's climate through the solution of fundamental equations describing the physics of the system.   In these models, a radiative perturbation associated with increase in a greenhouse gas (*radiative forcing)* triggers an initial warming;   complex responses follow involving for example enhanced evaporation of water vapor

from the ocean (a positive feedback, since water is a greenhouse gas), changes in cloud cover, and changes in the atmospheric or oceanic circulation. There is still considerable doubt regarding the ability of GCMs to simulate perturbations to climate, and indeed different GCMs show large disagreements in the predicted surface warmings resulting from a given increase in greenhouse gases. A major uncertainty is the response of cloud cover to the initial radiative forcing (section 7.5). Despite these problems, all GCMs tend to show a linear relationship between the initial radiative forcing and the ultimate perturbation to the surface temperature, the difference between models lying in the slope of that relationship. Because the radiative forcing can be calculated with some confidence, it provides a useful quantitative index to estimate and compare the potential of various atmospheric disturbances to affect climate.

7.4.1 Definition of radiative forcing

The radiative forcing caused by a change Δm in the atmospheric mass of a greenhouse gas X is defined as the resulting flux imbalance in the radiative budget for the Earth system. Consider a radiative model for the present-day atmosphere using observed or estimated values of all variables affecting the radiative budget including greenhouse gases, clouds, and aerosols (Figure 7-14, Step 1).
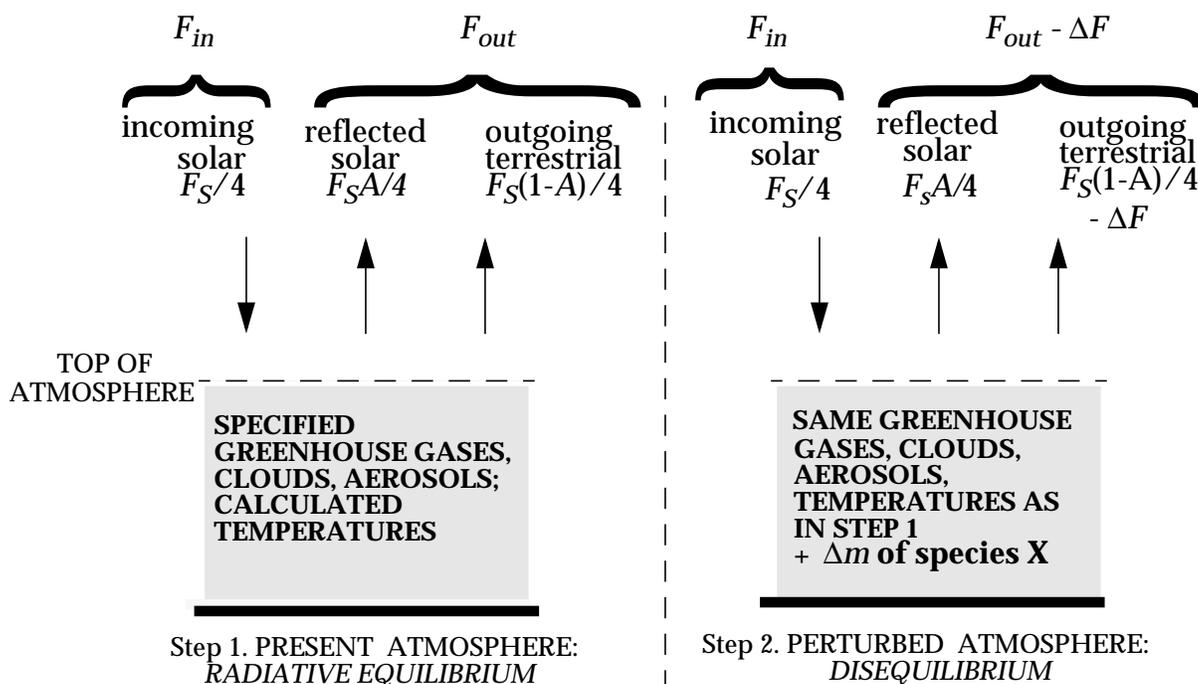

Figure 7-14 Calculation of the radiative forcing ΔF due to the addition Δm of a greenhouse gas. The "top of atmosphere" is commonly taken as the tropopause.

The model calculates the distribution of atmospheric temperatures necessary to achieve a global *radiative equilibrium* for the Earth system, that is, an exact balance between the incoming solar radiation flux at the top of the atmosphere ($F_S/4$), the outgoing solar radiation flux reflected by the Earth system ($F_S A/4$), and the terrestrial radiation flux emitted by the Earth system ($F_S(1\text{-}A)/4$). This equilibrium is necessary for a stable climate; as we will see below, even a small deviation would cause a large temperature perturbation. The model used for the calculation may be as simple as a 1-dimensional (vertical) formulation of radiative equilibrium, or as complicated as a GCM; the choice of model is not too important as long as the calculated temperature profiles are reasonably realistic.

Starting from this radiative equilibrium situation, we now perturb the equilibrium (Step 2) by adding Δm of species X, *keeping everything else constant* including temperature. If X is a greenhouse gas, then adding Δm will *decrease* the outgoing terrestrial flux at the top of the atmosphere by an amount ΔF; ΔF is the *radiative forcing* caused by increasing the mass of X by Δm. More generally, if F_{in} and F_{out} are the incoming and outgoing radiation fluxes in the radiative equilibrium calculation ($F_{in} = F_{out}$), then the radiative forcing associated with any perturbation to this equilibrium situation, and calculated with the same procedure as above, is defined as $\Delta F = F_{in} - F_{out}$.

Radiative forcing in research models is usually computed on the basis of the radiative perturbation at the tropopause rather than at the top of the atmosphere. That is, F_{in} and F_{out} in Step 2 are retrieved from the model at the tropopause after temperatures in the stratosphere have been allowed to readjust to equilibrium (temperatures in the troposphere are still held constant at their Step 1 values). The reason for this procedure is that a radiative perturbation in the stratosphere (as due, for example, to change in the stratospheric ozone layer) may have relatively little effect on temperatures at the Earth's surface due to the weak dynamical coupling between the stratosphere and the troposphere.

7.4.2 Application

The radiative forcing is a relatively simple quantity to calculate. By computing the radiative forcings associated with changes in emissions of individual greenhouse gases, we can assess and compare the potential climate effects of different gases and make

policy decisions accordingly. Figure 7-15, taken from a recent report from the Intergovernmental Panel on Climate Change (IPCC), gives the radiative forcings caused by changes in different greenhouse gases and other atmospheric variables since year 1850. Note that the anthropogenic radiative forcing from greenhouse gases is much larger than the natural forcing from change in solar intensity. Aerosols may induce a large negative forcing which we will discuss in chapter 8.
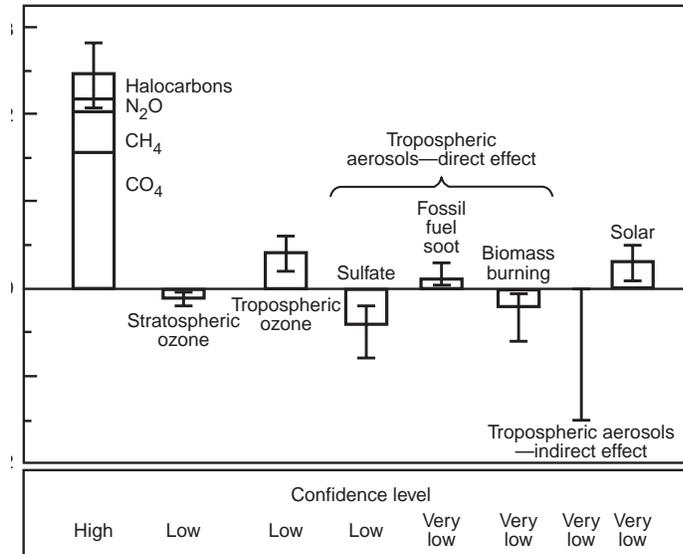

Figure 7-15 Globally averaged radiative forcing due to changes in greenhouse gases, aerosols, and solar activity from year 1850 to today. From *Climate Change 1994,* Intergovernmental Panel on Climate Change, Cambridge University Press, New York ,1995.

There is presently much interest in developing an international environmental policy aimed at greenhouse gas emissions. One must relate quantitatively the anthropogenic emission of a particular gas to the resulting radiative forcing. The index used is the global warming potential (GWP). The GWP of gas X is defined as the radiative forcing resulting from an instantaneous 1-kg injection of X into the atmosphere relative to the radiative forcing from an instantaneous 1-kg injection of CO_2:

$$GWP = \frac{\int_{t_o}^{t_o + \Delta t} \Delta F_{1\,kg\,X}\,dt}{\int_{t_o}^{t_o + \Delta t} \Delta F_{1\,kg\,CO2}\,dt} \qquad (7.17)$$

The forcing is integrated over a time horizon Δt starting from the time of injection t_0, and allowing for decay of the injected gas over that time horizon. One accounts in this manner for greater persistence of the radiative forcing for gases with long lifetimes.

Table 7-1 Global warming potentials from the instantaneous injection of 1 kg of a trace gas, relative to carbon dioxide

Gas	Lifetime, years	Global warming potential over integration time horizon		
		20 years	100 years	500 years
CO_2	~100	1	1	1
CH_4	10	62	25	8
N_2O	120	290	320	180
CFC-12	102	7900	8500	4200
HCFC-123	1.4	300	93	29
SF_6	3200	16500	24900	36500

Table 7-1 lists GWPs for several greenhouse gases and different time horizons. The synthetic gases CFCs, hydrofluorocarbons (HFCs) such as HCFC-123, and SF_6 have large GWPs because they absorb in the atmospheric window. The GWP of HFCs is less than that of CFCs because HFCs have shorter atmospheric lifetimes. Molecule for molecule, CO_2 is less efficient than other greenhouse gases because its atmospheric concentration is high and hence its absorption bands are nearly saturated. From Table 7-1 we see that over a 100-year time horizon, reducing SF_6 emissions by 1 kg is as effective from a greenhouse perspective as reducing CO_2 emissions by 24,900 kg. Such considerations are important in designing control strategies to meet regulatory goals!

7.4.3 Radiative forcing and surface temperature

We still need to relate the radiative forcing to change in the Earth's surface temperature, which is what we ultimately care about. Such a relationship can be derived using our simple 1-layer model for the atmosphere in section 7.3.2. In this model, the outgoing terrestrial flux for the initial atmosphere in radiative equilibrium

(Step 1) is $(1-f/2)\sigma T_o^4$, where f is the absorption efficiency of the atmospheric layer and T_o is the surface temperature (equation *(7.15)*). Increasing the abundance of a greenhouse gas by Δm corresponds to an increase Δf of the absorption efficiency. Thus the outgoing terrestrial flux for the perturbed atmosphere (Step 2) is $(1-(f+\Delta f)/2)\sigma T_o^4$. By definition of the radiative forcing ΔF,

$$\Delta F = \left(1 - \frac{f}{2}\right)\sigma T_o^4 - \left(1 - \frac{f+\Delta f}{2}\right)\sigma T_o^4 = \frac{\Delta f}{2}\sigma T_o^4 \qquad (7.18)$$

Let us now assume that the perturbation Δf is maintained for some time. Eventually, a new equilibrium state is reached where the surface temperature has increased by ΔT_o from its initial state. Following *(7.15)*, the new radiative equilibrium is defined by

$$\frac{F_S(1-A)}{4} = \left(1 - \frac{f+\Delta f}{2}\right)\sigma(T_o + \Delta T_o)^4 \qquad (7.19)$$

For a sufficiently small perturbation,

$$(T_o + \Delta T_o)^4 \approx T_o^4 + 4T_o^3\Delta T_o \qquad (7.20)$$

Replacing *(7.15)* and *(7.20)* into *(7.19)* we obtain:

$$\Delta T_o = \frac{T_o\Delta f}{8\left(1 - \frac{f}{2}\right)} \qquad (7.21)$$

Replacing *(7.18)* into *(7.21)*, we obtain a relationship between ΔT_o and ΔF:

$$\Delta T_o = \lambda\Delta F \qquad (7.22)$$

where λ is the *climate sensitivity parameter:*

$$\lambda = \frac{1}{4\left(1 - \frac{f}{2}\right)\sigma T_o^3} \qquad (7.23)$$

Substituting numerical values yields $\lambda = 0.3 \text{ K m}^2 \text{ W}^{-1}$. Figure 7-15 gives a total radiative forcing of 2.5 W m^{-2} from increases in

greenhouse gases since 1850. From our simple model, this forcing implies a change $\Delta T_o = 0.8$ K in the Earth's surface temperature, somewhat higher than the observed global warming of 0.6 K. Simulations using general circulation models indicate values of λ in the range 0.3-1.4 K m^2 W^{-1} depending on the model; the effect is larger than in our simple model, in large part due to positive feedback from increase in atmospheric water vapor. The models tend to overestimate the observed increase in surface temperature over the past century, perhaps due to moderating influences from clouds and aerosols as discussed below and in chapter 8.

7.5 WATER VAPOR AND CLOUD FEEDBACKS

7.5.1 Water vapor

Water vapor is the most important greenhouse gas present in the Earth's atmosphere. Direct human perturbation to water vapor (as from combustion or agriculture) is negligibly small compared to the large natural source of water vapor from the oceans. However, water vapor can provide a strong positive feedback to global warming initiated by perturbation of another greenhouse gas. Consider a situation in which a rise in CO_2 causes a small increase in surface temperatures. This increase will enhance the evaporation of water from the oceans. The greenhouse effect from the added water vapor will exacerbate the warming, evaporating more water from the oceans. Such amplification of the initial CO_2 forcing could conceivably lead to a *runaway greenhouse effect* where the oceans totally evaporate to the atmosphere and the surface temperature reaches exceedingly high values. Such a runaway greenhouse effect is thought to have happened in Venus's early history (the surface temperature of Venus exceeds 700 K). It cannot happen on Earth because accumulation of water vapor in the atmosphere results in the formation of clouds and precipitation, returning water to the surface.

To understand the difference between Venus and the Earth, we examine the early evolution of the temperature on each planet in the context of the phase diagram for water, as shown in Figure 7-16. Before the planets acquired their atmospheres, their surface temperatures were the same as their effective temperatures. The albedoes were low because of the lack of clouds or surface ice, and values of 0.15 are assumed for both planets. The resulting effective temperatures are somewhat higher than the values calculated in section 7.2. As water gradually outgassed from the planets' interiors and accumulated in the atmosphere, the greenhouse effect

increased surface temperatures. On Earth, the saturation water vapor pressure of water was eventually reached (Figure 7-16) at which point the water precipitated to form the oceans. On Venus, by contrast, the saturation water vapor pressure was never reached; oceans did not form and water vapor continued to accumulate in the atmosphere, resulting in a runaway greenhouse effect. The distance of the Earth from the Sun was critical in preventing this early runaway greenhouse effect.
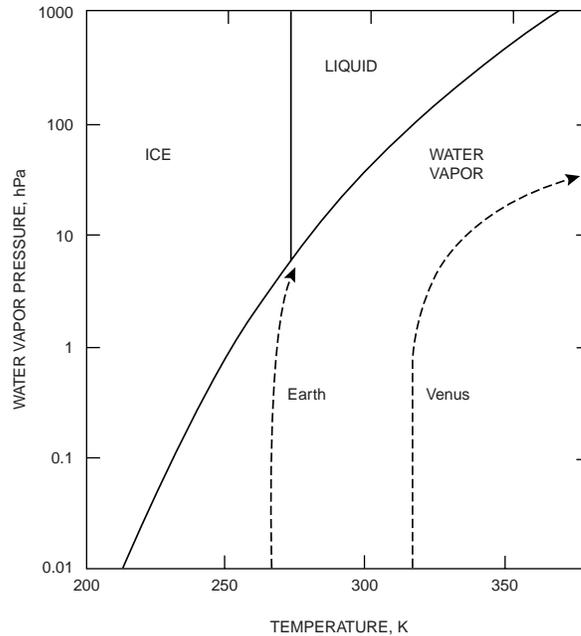

Figure 7-16 Evolution of temperatures in the early atmospheres of Venus and Earth (dashed lines), superimposed on the phase diagram of water.

7.5.2 Clouds

Feedbacks associated with changes in cloud cover represent the largest uncertainty in current estimates of climate change. Clouds can provide considerable negative feedback to global warming. We find from Figure 7-14 that the radiative forcing ΔF from an increase ΔA in the Earth's albedo is

$$\Delta F = -\frac{F_S \Delta A}{4} \tag{7.24}$$

An increase in albedo of 0.007 (or 2.6%) since preindustrial times would have caused a negative radiative forcing $\Delta F = -2.5$ W m^{-2}, canceling the forcing from the concurrent rise in greenhouse gases. Such a small increase in albedo would not have been observable. We might expect, as water vapor concentrations increase in the

atmosphere, that cloud cover should increase. However, that is not obvious. Some scientists argue that an increase in water vapor would in fact make clouds more likely to precipitate and therefore *decrease* cloud cover.

To further complicate matters, clouds not only increase the albedo of the Earth, they are also efficient absorbers of IR radiation and hence contribute to the greenhouse effect. Whether a cloud has a net heating or cooling effect depends on its temperature. High clouds (such as cirrus) cause net heating, while low clouds (such as stratus) cause net cooling. This distinction can be understood in terms of our one-layer greenhouse model. Inserting a high cloud in the model is like adding a second atmospheric layer; it enhances the greenhouse effect. A low cloud, however, has a temperature close to that of the surface due to transport of heat by convection. As a result it radiates almost the same energy as the surface did before the cloud formed, and there is little greenhouse warming .

7.6 OPTICAL DEPTH

The absorption or scattering of radiation by an optically active medium such as the atmosphere is measured by the *optical depth* δ of the medium. We have seen above how gas molecules absorb radiation; they also *scatter* radiation (that is, change its direction of propagation without absorption) but this scattering is inefficient at visible and IR wavelengths because of the small size of the gas molecules relative to the wavelength. Scattering is important for aerosols, which we will discuss in the next chapter. Consider in the general case a thin slab *[x, x+dx]* of an optically active medium absorbing or scattering radiation (Figure 7-17):
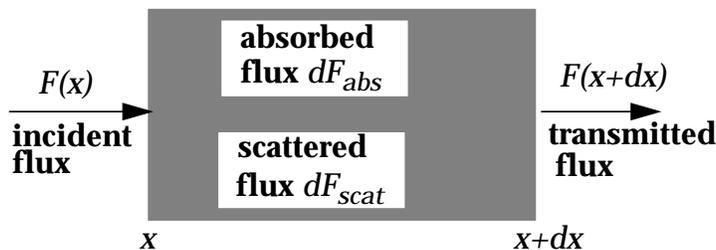

Figure 7-17 Transmission of radiation through an elemental slab

A radiation beam of flux $F(x)$ perpendicular to the surface of the slab may be absorbed (dF_{abs}), scattered (dF_{scat}), or transmitted through the slab without experiencing absorption or scattering ($F(x+dx)$):

$$F(x + dx) = F(x) - dF_{abs} - dF_{scat} \qquad (7.25)$$

We expect dF_{abs} and dF_{scat} to be proportional to $F(x)$, dx, and the number density n of the absorber or scatterer in the slab. We therefore introduce an *absorption cross-section* (σ_{abs}) and a *scattering cross-section* (σ_{scat}) which are intrinsic properties of the medium:

$$dF_{abs} = n\sigma_{abs}F(x)dx$$
$$dF_{scat} = n\sigma_{scat}F(x)dx \qquad (7.26)$$

Note that σ_{abs} and σ_{scat} have units of cm^2 molecule^{-1}, hence the "cross-section" terminology. Replacing *(7.26)* into *(7.25)*:

$$dF = F(x + dx) - F(x) = -n(\sigma_{abs} + \sigma_{scat})Fdx \qquad (7.27)$$

To calculate the radiation transmitted through a slab of length L, we integrate *(7.27)* by separation of variables:

$$F(L) = F(0)\exp[-n(\sigma_{abs} + \sigma_{scat})L] \qquad (7.28)$$

Thus the radiation decays exponentially with propagation distance through the slab. We define $\delta = n(\sigma_{abs} + \sigma_{scat})L$ as the *optical depth* of the slab:

$$\delta = \ln\frac{F(0)}{F(L)} \qquad (7.29)$$

such that $F(L) = F(0)e^{-\delta}$ is the flux transmitted through the slab. For a slab with both absorbing and scattering properties, one can decompose δ as the sum of an *absorption optical depth* ($\delta_{abs} = n\sigma_{abs}L$) and a *scattering optical depth* ($\delta_{scat} = n\sigma_{scat}L$). If the slab contains k different types of absorbers or scatterers, the total optical depth δ_T is obtained by adding the contributions from all species:

$$\delta_T = \sum_k \delta_i = \sum_k n_i(\sigma_{abs,\,i} + \sigma_{scat,\,i})L \qquad (7.30)$$

Absorption or scattering is more efficient if the radiation beam falls on the slab with a slant angle θ relative to the perpendicular, because the radiation then travels over a longer path inside the slab (Figure 7-18). The physical path of the beam through the slab is $L/$

cosθ, and the *optical path* is δ/cosθ:

$$F(L) \ = \ F(0)e^{-\frac{\delta}{\cos\theta}} \qquad\qquad (7.31)$$

**incident
flux**
F(0)

θ

$L/\cos\theta$

θ **transmitted
flux** $F(L) = F(0)e^{-\delta/\cos\theta}$
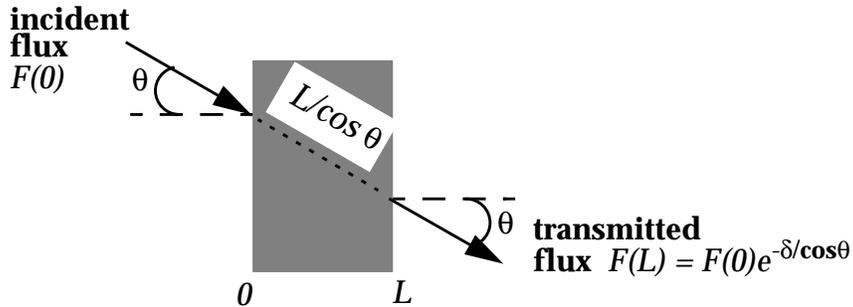
0 *L*

Figure 7-18 Effect of incident angle on the transmission of radiation through a slab

Further reading:

Goody, R., *Principles of Atmospheric Physics and Chemistry,* **Oxford University Press, New York, 1995.** Radiative transfer.

Houghton, J.T., *The Physics of Atmospheres,* **2nd ed., Cambridge University Press, New York, 1986.** Blackbody radiation, gray atmosphere model.

Intergovernmental Panel of Climate Change, *Climate Change 1994,* **Cambridge University Press, 1995.** Increases in greenhouse gases, radiative forcing.

Levine, I.N., *Physical Chemistry,* **4th ed., McGraw-Hill, New York, 1995.** Spectroscopy.